Acta Cryst E CRYSTALLOGRAPHIC COMMUNICATIONS

ISSN 2056-9890

Synthesis and crystal structure of *catena*-poly-[cobalt(II)-di-μ-chlorido-μ-pyridazine-κ^2N^1:N^2]

Christian Näther* and Inke Jess

Institut für Anorganische Chemie, Universität Kiel, Max-Eyth.-Str. 2, 24118 Kiel, Germany. *Correspondence e-mail: cnaether@ac.uni-kiel.de

Received 7 August 2023
Accepted 9 August 2023

Edited by W. T. A. Harrison, University of Aberdeen, United Kingdom

Keywords: synthesis; crystal structure; one-dimensional coordination compound.

CCDC reference: 2287781

Supporting information: this article has supporting information at journals.iucr.org/e

The reaction of cobalt dichloride hexahydrate with pyridazine leads to the formation of crystals of the title compound, $[CoCl_2(C_4H_4N_2)]_n$. This compound is isotypic to a number of compounds with other divalent metal ions. Its asymmetric unit consists of a Co^{2+} atom (site symmetry 2/*m*), a chloride ion (site symmetry *m*) and a pyridazine molecule (all atoms with site symmetry *m*). The Co^{2+} cations are coordinated by four chloride anions and two pyridazine ligands, generating *trans*-CoN_4Cl_2 octahedra, and are linked into [010] chains by pairs of μ-1,1-bridging chloride anions and bridging pyridazine ligands. In the crystal structure, the pyridazine ligands of neighboring chains are stacked onto each other, indicating π–π interactions. Powder X-ray diffraction proves that a pure crystalline phase was obtained. Differential thermonalysis coupled to thermogravimetry (DTA–TG) reveal that decomposition is observed at about 710 K. Magnetic measurements indicate low-temperature metamagnetic behavior as already observed in a related compound.

1. Chemical context

Mono-periodic coordination polymers have always attracted much interest because of their versatile physical properties (Leong & Vittal, 2011; Mas-Ballesté *et al.*, 2010; Cernák *et al.*, 2002; Chen & Suslick, 1993; Khlobystov *et al.*, 2001). This includes mono-periodic coordination polymers, which can show a variety of different magnetic properties including single-chain magnetic behavior (Lescouëzec *et al.*, 2005; Rams *et al.*, 2020; Werner *et al.*, 2015; Sun *et al.*, 2010; Dhers *et al.*, 2015). In this context, of interest are coordination polymers based on transition-metal halides in which the metal cations are linked by pairs of μ-1,1-bridging halide anions into chains. The most prominent cations such as Mn^{II}, Fe^{II}, Co^{II} or Ni^{II} are mostly octahedrally coordinated, which means that for the synthesis of compounds with chain structures, mono-coordinating ligands must be used and several such compounds have already been reported in the literature (Foner *et al.*, 1975, 1978; Qin *et al.*, 2015; Zheng *et al.*, 2010). Compounds with a chain structure may also be observed if ligands such as tetrazole or pyridazine derivatives are used, in which the nitrogen donor atoms are adjacent. In this case, the chain structure remains unchanged and the co-ligand bridges two neighboring metal cations within the chain (Ivashkevich *et al.*, 2009; Masciocchi *et al.*, 1994; Thomas & Ramanan, 2016). In this context, Masciocchi and coworkers have reported on compounds with the composition $NiX_2(C_4H_4N_2)$ where $C_4H_4N_2$ = pyridazine (1,2-diazine) with *X* = Cl, Br that were structurally characterized by X-ray powder diffraction (Masciocchi *et al.*, 1994). In these structures, the Ni^{II} cations are linked by pairs of halide anions into chains and within the

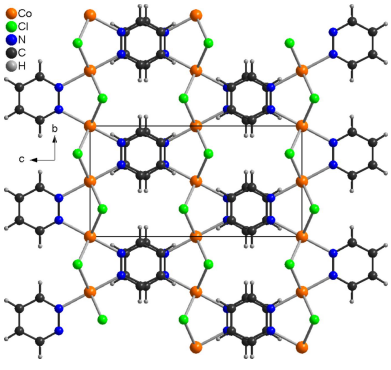

chains, neighboring Ni^{II} cations are additionally bridged by the pyridazine ligands.

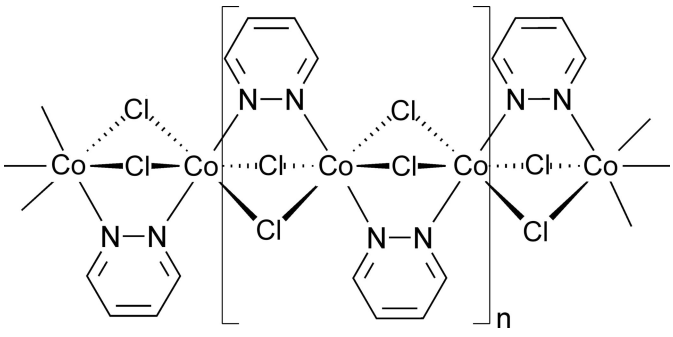

We are also interested in coordination polymers in which the metal cations are linked by small-sized anionic ligands into one- or two-dimensional networks. In the beginning, we investigated compounds based on Cu^{I} cations and halide anions with additional N-donor coligands because we have found that, upon heating, they lose their coligands in a stepwise manner and transform into new coligand-deficient compounds that show condensed copper–halide networks (Näther & Jess, 2004; Näther *et al.*, 2001, 2007). Later we found that this synthetic procedure can also be used for compounds with divalent cations such as Cd^{II} (Näther *et al.*, 2017). In the course of this project, we also became interested in metal-halide compounds with paramagnetic metal cations and as part of these investigations, we reacted $CoCl_2$ with pyridazine and obtained a compound with the composition $CoCl_2(C_4H_4N_2)$. No entry was found in the Cambridge Structural Database (CSD, version 5.43, last update March 2023; Groom *et al.*, 2016) and therefore this compound was characterized by single-crystal X-ray diffraction. Later we found that this compound had already been characterized by X-ray powder diffraction and it was concluded that it is isotypic to its Ni^{II} counterpart (Masciocchi *et al.*, 1994), which we found is the case.

2. Structural commentary

The reaction of $CoCl_2{\cdot}6H_2O$ with pyridazine in water in a sealed vessel at 388 K leads to the formation of single crystals of the title compound $CoCl_2(C_4H_4N_2)$. This compound is isotypic to its Mn^{II}, Fe^{II} and Ni^{II} analogs with chloride and bromide as counter-anions, already reported in the literature (Masciocchi *et al.*, 1994). The asymmetric unit consists of one cobalt(II) cation located at (1/4, 1/4, 1/4) on the intersection point of a twofold screw axis and a mirror plane (Wyckoff site 4*c*, site symmetry 2/*m*), as well as one chloride anion at (1/2, *y*, *z*) that is situated on a mirror plane on Wyckoff site 8*h*. The asymmetric unit also contains half a pyridazine ligand with all atoms located at (*x*, 1/4, *z*) on Wyckoff position 8*i* (*m* site symmetry): the complete $C_4H_4N_2$ ligand is generated by a second mirror plane at x = 1/2 (Fig. 1). The Co^{II} cations are octahedrally coordinated by four chloride anions and two pyridazine ligands and from the bond lengths and angles, it is

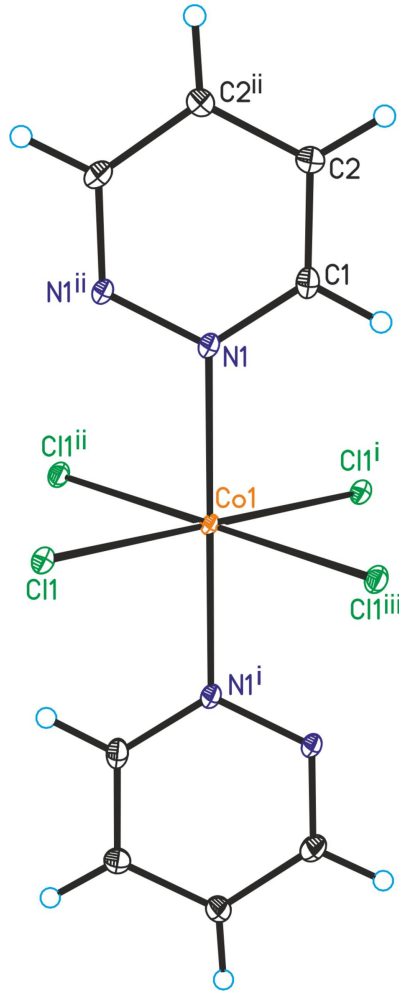

Figure 1
Crystal structure of the title compound with labeling and displacement ellipsoids drawn at the 50% probability level. Symmetry codes for the generation of equivalent atoms: (i) $-x+1, \frac{3}{2}-y, z$; (ii) $-x+1, -y+1, -z+1$; (iii) $x, -\frac{1}{2}+y, -z+1$.

obvious that the octahedra are slightly distorted (Table 1). The Co^{II} cations are linked by pairs of μ-1,1-bridging chloride anions into chains that propagate in the *b*-axis direction (Fig. 2). The pyridazine ligands also act as bridging ligands, each connecting two neighboring Co^{II} cations. Within the chains, all of the pyridazine ligands are coplanar. The intra-chain Co···Co distance is 3.3443 (3) Å.

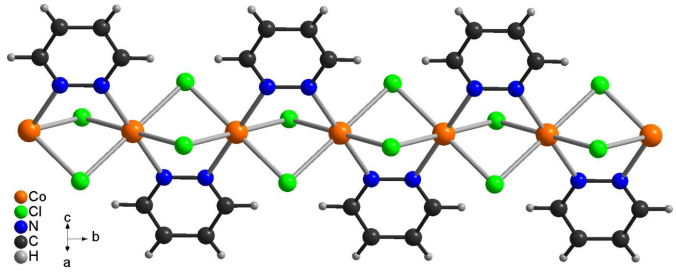

Figure 2
Fragment of a [010] polymeric chain in the title compound.

Table 1
Selected geometric parameters (Å, °).

Co1—N1	2.1282 (19)	Co1—Cl1	2.4626 (4)
N1—Co1—N1^{i}	180.0	Cl1—Co1—Cl1^{i}	180.0
N1—Co1—Cl1	87.21 (4)	Cl1—Co1—Cl1^{ii}	83.66 (2)
N1^{i}—Co1—Cl1	92.79 (4)	Cl1^{i}—Co1—Cl1^{ii}	96.34 (2)

Symmetry codes: (i) $-x+\frac{1}{2}, -y+\frac{1}{2}, -z+\frac{1}{2}$; (ii) $-x+1, -y+\frac{1}{2}, z$.

3. Supramolecular features

In the crystal structure of the title compound, the chains propagate in the *b*-axis direction and are arranged in such a way that neighboring pyridazine ligands are perfectly stacked onto each other, forming columns along the crystallographic *a* axis (Fig. 3). The angle between two neighboring pyridazine ligands is 180° and the distance between their centroids is 3.6109 (1) Å (slippage = 0.264 Å), indicating π–π stacking interactions. One very weak C—H···Cl hydrogen bond (Table 2) is observed.

4. Database survey

Many compounds of the general formula $MX_2(C_4H_4N_2)$ (M = transition metal and X = halide anion have already been reported in the Cambridge Structural Database but there are no hits for cobalt. The compounds with $NiCl_2$ (CSD refcode POPCIG) and $NiBr_2$ (POPCOM) were structurally characterized by Rietveld refinements using laboratory X-ray powder diffraction data (Masciocchi *et al.*, 1994). In this contribution, the compounds with Mn, Fe, Co, Cu and Zn with chloride and bromide as anions were also synthesized and from their powder patterns, the lattice parameters were determined, which indicate that the compounds with Mn, Fe and Co are isotypic to the Ni compounds; this is not the case for the compounds with Cu and Zn (Masciocchi *et al.*, 1994). Our determination definitively proves that the title compound is isotypic to its Ni analog. The compounds $MCl_2(C_4H_4N_2)$ with Mn (LANJEQ), Fe (LANJAM) were later determined by single-crystal X-ray diffraction, and their magnetic properties were also investigated (Yi *et al.*, 2002).

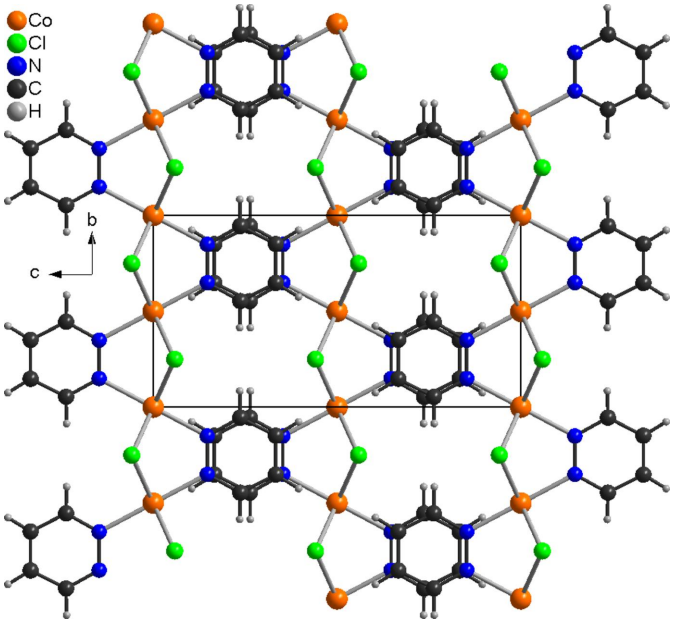

Figure 3
Arrangement of the chains in the crystal structure of the title compound with view along the crystallographic *a*-axis direction.

Table 2
Hydrogen-bond geometry (Å, °).

D—H···A	D—H	H···A	D···A	D—H···A
C2—H2···Cl1^{iii}	0.95	2.97	3.574 (2)	123

Symmetry code: (iii) $x-\frac{1}{2}, y-\frac{1}{2}, z+\frac{1}{2}$.

With copper, additional compounds were investigated by single-crystal X-ray diffraction, including $CuCl_2(C_4H_4N_2)$ (JEFFOS; Thomas & Ramanan, 2016) and $CuBr_2$(pyridiazine) (JEFFUY; Thomas & Ramanan, 2016). However, most compounds are reported with Cu^{I}, including $CuI(C_4H_4N_2)$ (CAQXAT; Kromp & Sheldrick, 1999, and CAQXAT01; Thomas & Ramanan, 2016), $CuBr(C_4H_4N_2)$ (CAQXEX; Kromp & Sheldrick, 1999, and CAQXEX01 and 02; Thomas & Ramanan, 2016), $Cu_2I_2(C_4H_4N_2)$ (CAQXIB; Kromp & Sheldrick, 1999), $Cu_2Cl_2(C_4H_4N_2)$ (CAQXOH; Kromp & Sheldrick, 1999, and CAQXOH01 and 02; Thomas & Ramanan, 2016), two modifications of $CuCl(C_4H_4N_2)$ (EKINOB and EKINUH; Näther & Jess, 2003, and EKINUH01; Thomas & Ramanan, 2016), $Cu_2Br_2(C_4H_4N_2)$ (EKIPAP; Näther & Jess, 2003, and EKIPAP01; Thomas & Ramanan, 2016).

With diamagnetic Zn^{II}, three compounds are reported, namely $ZnI_2(C_4H_4N_2)_2$ (MENSUU; Bhosekar *et al.*, 2006*a*), $ZnBr_2(C_4H_4N_2)_2$ (VEMBEV; Bhosekar *et al.*, 2006*b*) and three modifications of $ZnCl_2(C_4H_4N_2)_2$ (YAFYOU, YAFYOU01, YAFYOU02 and YAFYOU03; Pazderski *et al.*, 2004*a* and Bhosekar *et al.*, 2007). Finally, the Cd compounds $CdCl_2(C_4H_4N_2)$ (AZABUY; Pazderski *et al.*, 2004*b*), $CdBr_2(C_4H_4N_2)$ and $CdI_2(C_4H_4N_2)$ have also been reported (refcodes to be assigned; Näther & Jess, 2023).

5. Physical characterization

The experimental powder pattern of the title compound agrees closely with that calculated from the single crystal data, which proves that a pure compound was obtained (Fig. S1). The thermal properties were investigated by differential thermoanalysis and thermogravimetry (DTA–TG) under an air atmosphere. Upon heating, only one mass loss is observed, which is accompanied by an endothermic event in the DTA curve (Fig. S2). The experimental mass loss of 27.4% is much lower than that calculated for the removal of one pyridazine ligand (38.2%), indicating that the pyridazine ligands are not completely removed. This is supported by the fact that the TG curve still decreases upon further heating. In the DTA curve, a successive endothermic and exothermic event is observed, which points to the decomposition of this compound (Fig. S2).

Table 3
Experimental details.

Crystal data	
Chemical formula	$[CoCl_2(C_4H_4N_2)]$
M_r	209.92
Crystal system, space group	Orthorhombic, *Imma*
Temperature (K)	100
a, b, c (Å)	6.6935 (1), 7.2024 (1), 12.7978 (2)
V (Å^3)	616.97 (2)
Z	4
Radiation type	Cu $K\alpha$
μ (mm^{-1})	28.91
Crystal size (mm)	0.1 × 0.08 × 0.08
Data collection	
Diffractometer	XtaLAB Synergy, Dualflex, HyPix
Absorption correction	Multi-scan (*CrysAlis PRO*; Rigaku OD, 2022)
T_{min}, T_{max}	0.316, 1.000
No. of measured, independent and observed [$I > 2\sigma(I)$] reflections	3164, 395, 386
R_{int}	0.027
(sin $\theta/\lambda)_{max}$ (Å^{-1})	0.639
Refinement	
$R[F^2 > 2\sigma(F^2)]$, $wR(F^2)$, S	0.020, 0.058, 1.07
No. of reflections	395
No. of parameters	30
H-atom treatment	H-atom parameters constrained
$\Delta\rho_{max}$, $\Delta\rho_{min}$ (e Å^{-3})	0.64, −0.34

Computer programs: *CrysAlis PRO* (Rigaku OD, 2022), *SHELXT2014* (Sheldrick, 2015*a*), *SHELXL2016* (Sheldrick, 2015*b*), *DIAMOND* (Brandenburg, 1999) and *publCIF* (Westrip, 2010).

The title compounds were also characterized by magnetic measurements. The temperature dependence of the susceptibility was measured in the range 2–300 K under an applied magnetic field of 1000 Oe. Upon cooling, a maximum is observed at 3.0 K, indicating an antiferromagnetic transition (Fig. S3). The data were analyzed using a Curie–Weiss law, leading to a magnetic moment of 5.0 μ_B, which is higher than expected for a Co^{II} cation in a high-spin $3d^7$ configuration. The Weiss constant of −8 K suggests predominant antiferromagnetic interactions, but it must be kept in mind that these values are frequently too high because of the strong spin–orbit coupling of Co^{II}. Additional field-dependent measurements at 2 K indicate metamagnetic behavior with no saturation even at high fields, as previously observed for the linear chain compound $CoCl_2(C_4H_4N_2)_2$ (Fig. S4; Foner *et al.*, 1975).

6. Synthesis and crystallization

Synthesis

$CoCl_2{\cdot}6H_2O$ and pyridazine were purchased from Sigma Aldrich and pyridazine from Alfa Aesar. All chemicals were used without further purification.

Pink-colored crystals were obtained by the reaction of 1 mmol of $Co(NCS)_2$ (237.9 mg) and 1 mmol (72 µl) of pyridazine in 1 ml of demineralized water. The reaction mixture was heated in a sealed glass vessel at 388 K for 2 d, leading to the formation of crystals suitable for single-crystal X-ray analysis. An IR spectrum of the title compound can be found in Fig. S5.

Experimental details

The IR spectrum was measured using an ATI Mattson Genesis Series FTIR Spectrometer, control software: WINFIRST, from ATI Mattson.

The PXRD measurement was performed with Cu $K\alpha_1$ radiation (λ = 1.540598 Å) using a Stoe Transmission Powder Diffraction System (STADI P) equipped with a MYTHEN 1K detector and a Johansson-type Ge(111) monochromator.

Thermogravimetry and differential thermoanalysis (TG–DTA) measurements were performed in a dynamic air atmosphere in Al_2O_3 crucibles using a STA-PT 1000 thermobalance from Linseis. The instrument was calibrated using standard reference materials.

Magnetic measurements were performed using a Quantum Design PPMS equipped with a 7 T magnet, using samples mounted in a gelatine capsule.

7. Refinement

Crystal data, data collection and structure refinement details are summarized in Table 3. The C—H hydrogen atoms were positioned with idealized geometry and refined as riding atoms with $U_{iso}(H) = 1.2\ U_{eq}(C)$.

Acknowledgements

Financial support by the State of Schleswig-Holstein is gratefully acknowledged.

References

Bhosekar, G., Jess, I., Havlas, Z. & Näther, C. (2007). *Cryst. Growth Des.* **7**, 2627–2634.
Bhosekar, G., Jess, I. & Näther, C. (2006*a*). *Acta Cryst.* E**62**, m2073–m2074.
Bhosekar, G., Jess, I. & Näther, C. (2006*b*). *Acta Cryst.* E**62**, m1859–m1860.
Brandenburg, K. (1999). *DIAMOND*. Crystal Impact GbR, Bonn, Germany.
Cernák, J., Orendác, M., Potocnák, I., Chomic, J., Orendácová, A., Skorsepa, J. & Feher, A. (2002). *Coord. Chem. Rev.* **224**, 51–66.
Chen, C. T. & Suslick, K. S. (1993). *Coord. Chem. Rev.* **128**, 293–322.
Dhers, S., Feltham, H. L. C. & Brooker, S. (2015). *Coord. Chem. Rev.* **296**, 24–44.
Foner, S., Frankel, R. B., Reiff, W. M., Little, B. F. & Long, G. J. (1975). *Solid State Commun.* **16**, 159–161.
Foner, S., Frankel, R. B., Reiff, W. M., Wong, H. & Long, G. J. J. (1978). *Chem. Phys.* **68**, 4781–4783.
Groom, C. R., Bruno, I. J., Lightfoot, M. P. & Ward, S. C. (2016). *Acta Cryst.* B**72**, 171–179.
Ivashkevich, L. S., Lyakhov, A. S., Mosalkova, A. P., Gaponik, P. N. & Ivashkevich, O. A. (2009). *Acta Cryst.* E**65**, m236.
Khlobystov, A. N., Blake, A. J., Champness, N. R., Lemenovskii, D. A., Majouga, A. G., Zyk, N. V. & Schröder, M. (2001). *Coord. Chem. Rev.* **222**, 155–192.
Kromp, T. & Sheldrick, W. S. (1999). *Z. Naturforsch.* **54**, 1175–1180.
Leong, W. L. & Vittal, J. J. (2011). *Chem. Rev.* **111**, 688–764.
Lescouëzec, R., Toma, L. M., Vaissermann, J., Verdaguer, M., Delgado, F. S., Ruiz-Pérez, C., Lloret, F. & Julve, M. (2005). *Coord. Chem. Rev.* **249**, 2691–2729.
Mas-Ballesté, R., Gómez-Herrero, J. & Zamora, F. (2010). *Chem. Soc. Rev.* **39**, 4220–4223.

Masciocchi, N., Cairati, O., Carlucci, L., Ciani, G., Mezza, G. & Sironi, A. (1994). *J. Chem. Soc. Dalton Trans.* pp. 3009–3015.
Näther, C., Bhosekar, G. & Jess, I. (2007). *Inorg. Chem.* **46**, 8079–8087.
Näther, C. & Jess, I. (2004). *Eur. J. Inorg. Chem.* pp. 2868–2876.
Näther, C., Jess, I. & Greve, J. (2001). *Polyhedron*, **20**, 1017–1022.
Näther, C. & Jess, I. (2003). *Inorg. Chem.* **42**, 2968–2976.
Näther, C. & Jess, I. (2023). *Acta Cryst.* E**79**, 302–307.
Näther, C., Jess, I., Germann, L. S., Dinnebier, R. E., Braun, M. & Terraschke, H. (2017). *Eur. J. Inorg. Chem.* pp. 1245–1255.
Pazderski, L., Szlyk, E., Wojtczak, A., Kozerski, L., Sitkowski, J. & Kamieński, B. (2004*b*). *J. Mol. Struct.* **697**, 143–149.
Pazderski, L., Szłyk, E., Wojtczak, A., Kozerski, L. & Sitkowski, J. (2004*a*). *Acta Cryst.* E**60**, m1270–m1272.
Qin, L., Zhang, Z., Zheng, Z., Speldrich, M., Kögerler, P., Xue, W., Wang, B. Y., Chen, X. M. & Zheng, Y. Z. (2015). *Dalton Trans.* **44**, 1456–1464.
Rams, M., Jochim, A., Böhme, M., Lohmiller, T., Ceglarska, M., Rams, M. M., Schnegg, A., Plass, W. & Näther, C. (2020). *Chem. Eur. J.* **26**, 2837–2851.
Rigaku OD (2022). *CrysAlis PRO*. Rigaku Oxford Diffraction.
Sheldrick, G. M. (2015*a*). *Acta Cryst.* A**71**, 3–8.
Sheldrick, G. M. (2015*b*). *Acta Cryst.* C**71**, 3–8.
Sun, H. L., Wang, Z. M. & Gao, S. (2010). *Coord. Chem. Rev.* **254**, 1081–1100.
Thomas, J. & Ramanan, A. (2016). *J. Chem. Sci.* **128**, 1687–1694.
Werner, J., Tomkowicz, Z., Rams, M., Ebbinghaus, S. G., Neumann, T. & Näther, C. (2015). *Dalton Trans.* **44**, 14149–14158.
Westrip, S. P. (2010). *J. Appl. Cryst.* **43**, 920–925.
Yi, T., Chang, H. C. & Kitagawa, S. (2002). *Mol. Cryst. Liq. Cryst.* **376**, 283–288.
Zheng, Y. Z., Speldrich, M., Schilder, H., Chen, X. M. & Kögerler, P. (2010). *Dalton Trans.* **39**, 10827–10829.

supporting information

Acta Cryst. (2023). E**79**, 872-876 [https://doi.org/10.1107/S2056989023007065]

Synthesis and crystal structure of *catena*-poly[cobalt(II)-di-μ-chlorido-μ-pyridazine-$\kappa^2N^1{:}N^2$]

Christian Näther and Inke Jess

Computing details

Data collection: *CrysAlis PRO* (Rigaku OD, 2022); cell refinement: *CrysAlis PRO* (Rigaku OD, 2022); data reduction: *CrysAlis PRO* (Rigaku OD, 2022); program(s) used to solve structure: *SHELXT2014* (Sheldrick, 2015a); program(s) used to refine structure: *SHELXL2016* (Sheldrick, 2015b); molecular graphics: *DIAMOND* (Brandenburg, 1999); software used to prepare material for publication: *publCIF* (Westrip, 2010).

***catena*-poly[cobalt(II)-di-μ-chlorido-μ-pyridazine-$\kappa^2N^1{:}N^2$]**

Crystal data

$[CoCl_2(C_4H_4N_2)]$
M_r = 209.92
Orthorhombic, *Imma*
a = 6.6935 (1) Å
b = 7.2024 (1) Å
c = 12.7978 (2) Å
V = 616.97 (2) Å^3
Z = 4
$F(000)$ = 412
D_x = 2.260 Mg m^{-3}
Cu $K\alpha$ radiation, λ = 1.54184 Å
Cell parameters from 2503 reflections
θ = 6.9–78.2°
μ = 28.91 mm^{-1}
T = 100 K
Block, pink
0.1 × 0.08 × 0.08 mm

Data collection

XtaLAB Synergy, Dualflex, HyPix diffractometer
Radiation source: micro-focus sealed X-ray tube, PhotonJet (Cu) X-ray Source
Mirror monochromator
Detector resolution: 10.0000 pixels mm^{-1}
ω scans
Absorption correction: multi-scan (CrysAlis PRO; Rigaku OD, 2022)
T_{min} = 0.316, T_{max} = 1.000
3164 measured reflections
395 independent reflections
386 reflections with $I > 2\sigma(I)$
R_{int} = 0.027
θ_{max} = 80.2°, θ_{min} = 6.9°
h = −8→8
k = −8→8
l = −16→15

Refinement

Refinement on F^2
Least-squares matrix: full
$R[F^2 > 2\sigma(F^2)]$ = 0.020
$wR(F^2)$ = 0.058
S = 1.07
395 reflections
30 parameters
0 restraints
Primary atom site location: dual
Hydrogen site location: inferred from neighbouring sites
H-atom parameters constrained
$w = 1/[\sigma^2(F_o^2) + (0.039P)^2 + 0.9618P]$ where $P = (F_o^2 + 2F_c^2)/3$
$(\Delta/\sigma)_{max} < 0.001$
$\Delta\rho_{max}$ = 0.64 e Å^{-3}
$\Delta\rho_{min}$ = −0.34 e Å^{-3}

Extinction correction: SHELXL2016 (Sheldrick, 2015b), $Fc^*=kFc[1+0.001xFc^2\lambda^3/\sin(2\theta)]^{-1/4}$
Extinction coefficient: 0.0016 (3)

Special details

Geometry. All esds (except the esd in the dihedral angle between two l.s. planes) are estimated using the full covariance matrix. The cell esds are taken into account individually in the estimation of esds in distances, angles and torsion angles; correlations between esds in cell parameters are only used when they are defined by crystal symmetry. An approximate (isotropic) treatment of cell esds is used for estimating esds involving l.s. planes.

Fractional atomic coordinates and isotropic or equivalent isotropic displacement parameters (Å²)

	x	*y*	*z*	U_{iso}*/U_{eq}
Co1	0.250000	0.250000	0.250000	0.0069 (2)
Cl1	0.500000	0.47804 (8)	0.19118 (4)	0.0089 (2)
N1	0.3991 (3)	0.250000	0.39687 (15)	0.0082 (4)
C1	0.3025 (4)	0.250000	0.48765 (19)	0.0126 (5)
H1	0.160605	0.250000	0.486369	0.015*
C2	0.3973 (4)	0.250000	0.58452 (17)	0.0112 (5)
H2	0.323309	0.250000	0.647854	0.013*

Atomic displacement parameters (Å²)

	U^{11}	U^{22}	U^{33}	U^{12}	U^{13}	U^{23}
Co1	0.0036 (3)	0.0111 (3)	0.0062 (3)	0.000	−0.00030 (17)	0.000
Cl1	0.0060 (3)	0.0108 (3)	0.0099 (3)	0.000	0.000	0.00073 (17)
N1	0.0052 (9)	0.0107 (9)	0.0087 (8)	0.000	0.0001 (7)	0.000
C1	0.0076 (11)	0.0184 (12)	0.0118 (11)	0.000	0.0020 (10)	0.000
C2	0.0103 (12)	0.0142 (11)	0.0090 (11)	0.000	−0.0005 (9)	0.000

Geometric parameters (Å, º)

Co1—N1	2.1282 (19)	N1—C1	1.330 (3)
Co1—N1^{i}	2.1282 (19)	N1—N1^{ii}	1.350 (4)
Co1—Cl1	2.4626 (4)	C1—C2	1.393 (3)
Co1—Cl1^{i}	2.4626 (4)	C1—H1	0.9500
Co1—Cl1^{ii}	2.4626 (4)	C2—C2^{ii}	1.374 (5)
Co1—Cl1^{iii}	2.4626 (4)	C2—H2	0.9500
N1—Co1—N1^{i}	180.0	Cl1^{i}—Co1—Cl1^{iii}	83.66 (2)
N1—Co1—Cl1	87.21 (4)	Cl1^{ii}—Co1—Cl1^{iii}	180.0
N1^{i}—Co1—Cl1	92.79 (4)	Co1—Cl1—Co1^{ii}	85.611 (17)
N1—Co1—Cl1^{i}	92.79 (4)	C1—N1—N1^{ii}	119.10 (15)
N1^{i}—Co1—Cl1^{i}	87.21 (4)	C1—N1—Co1	122.93 (17)
Cl1—Co1—Cl1^{i}	180.0	N1^{ii}—N1—Co1	117.97 (5)
N1—Co1—Cl1^{ii}	87.21 (4)	N1—C1—C2	123.8 (3)
N1^{i}—Co1—Cl1^{ii}	92.79 (4)	N1—C1—H1	118.1
Cl1—Co1—Cl1^{ii}	83.66 (2)	C2—C1—H1	118.1

Cl1^{i}—Co1—Cl1^{ii}	96.34 (2)	C2^{ii}—C2—C1	117.11 (16)
N1—Co1—Cl1^{iii}	92.79 (4)	C2^{ii}—C2—H2	121.4
N1^{i}—Co1—Cl1^{iii}	87.21 (4)	C1—C2—H2	121.4
Cl1—Co1—Cl1^{iii}	96.34 (2)		

Symmetry codes: (i) −*x*+1/2, −*y*+1/2, −*z*+1/2; (ii) −*x*+1, −*y*+1/2, *z*; (iii) *x*−1/2, *y*, −*z*+1/2.

Hydrogen-bond geometry (Å, º)

D—H···*A*	*D*—H	H···*A*	*D*···*A*	*D*—H···*A*
C2—H2···Cl1^{iv}	0.95	2.97	3.574 (2)	123

Symmetry code: (iv) *x*−1/2, *y*−1/2, *z*+1/2.